Prediction of dynamic response of wind turbine towers in the parked condition

Nan Xu [a], Takeshi Ishihara [b]

[a] *The University of Tokyo, Tokyo, Japan, xu@bridge.t.u-tokyo.ac.jp*
[b] *The University of Tokyo, Tokyo, Japan, ishihara@bridge.t.u-tokyo.ac.jp*

1 INTRODUCTION

IEC 61400-1 (2005) requires that assessment of structural integrity by load calculations with reference to site specific conditions is necessary. Equivalent static method is adopted to estimate the design wind load on engineering structures by many design codes, in which the non-linear part of wind pressure is neglected. Therefore, for wind turbines exposed to high wind turbulence in areas with complex terrain like Japan, the design wind load may be underestimated, since contribution of the non-linear part of wind pressure is large and the response is non-Gaussian. Binh et al. (2008) derived the mean wind load which considers the non-linear part of wind pressure and proposed a non-Gaussian peak factor for the design of wind turbine towers. This model gives a good performance for the prediction of design wind load compared with conventional models.

Wind Energy Handbook (2001) and Binh's model are conducted for DLC 6.2 (loss of electrical network connection) in IEC 61400-1 (2005). In this abnormal case, the most unfavorable yaw angle of 0° or ±180° is chosen to calculate the design wind load (Ishihara et al. 2005a, 2005b). For 0° or ±180°, the drag force on the rotor is dominant and the lift force can be neglected. However, for DLC 6.1 (normal case for yaw control), the yaw angle range of 0°±180° shall be analyzed. Therefore, the wind load for arbitrary yaw angle should be calculated and the lift force on the rotor may become significant.

In this study, the wind load evaluation formulas of both along-wind direction and across-wind direction are proposed for arbitrary yaw angle. The complex integrals of some critical parameters are simplified in order to recognize the dominant influence factor and get a clear understanding of how the parameters vary with the size of wind turbine. A new non-Gaussian peak factor model is proposed for along-wind direction, which can be reduced to the conventional Gaussian form for a Gaussian case. A formula for the combination of along wind and across wind loads is proposed to calculate the design wind load, considering the correlation coefficient of wind responses in the two directions. Finally, the proposed formula is verified by FEM (finite element model) simulation.

2 WIND LOAD FOR ALONG-WIND DIRECTION

Equivalent static wind load evaluation formula is adopted to estimate the maximum wind load on wind turbines:

$$M_D = \overline{M_D} + g_D \cdot \sigma_{MD} = \overline{M_D} + g_D \sqrt{\sigma_{MRD}^2 + \sigma_{MBD}^2} \tag{1}$$

where $\overline{M_D}$ is the mean bending moment, g_D is the peak factor, σ_{MD} is the standard deviation which consists of a resonant part σ_{MRD} and a background part σ_{MBD}.

In the simplification of formulas, the tower height is assumed to be equal to the hub height. Wind velocity and turbulence intensity at the hub of the wind turbine are used as representative for that of the whole rotor. A uniform equivalent aerodynamic coefficient for the whole rotor is used instead of that varying with positions on the rotor. Since in wind load of wind turbine tower the effect of the first mode is dominant, only the first mode is

considered. The first modal frequency f and mode shape $\mu(r)$ for tower refer to Ishihara (2007).

2.1 *Mean bending moment*

The mean bending moment at the tower base can be calculated as:

$$\overline{M_D} = \int_{wt} \frac{1}{2}\rho C_D(r,\theta)c(r)U^2(r)\left[1+I_u^{\,2}(r)\right]rdr \tag{2}$$

where ρ is the air density, $C_D(r,\theta)$ is the drag aerodynamic coefficient, θ is yaw angle, $c(r)$ is the characteristic length of the element at position r, $U(r)$ is the mean wind velocity, $I_u(r)$ is the turbulence intensity in the along-wind direction, and wt denotes the areas which contribute to the mean bending moment at the tower base. To consider non-linear part of wind force, the term of $I_u^{\,2}(r)$ is taken into account to calculate the mean wind load.

A 400kW stall-regulated wind turbine is taken as an example. From Figure 1, it can be seen that compared to the underestimation of linear formula, the nonlinear formula of this study gives more accurate mean bending moment, especially for high turbulence intensity the calculated load is increased by more than 6%, and the error is limited to less than 3%.

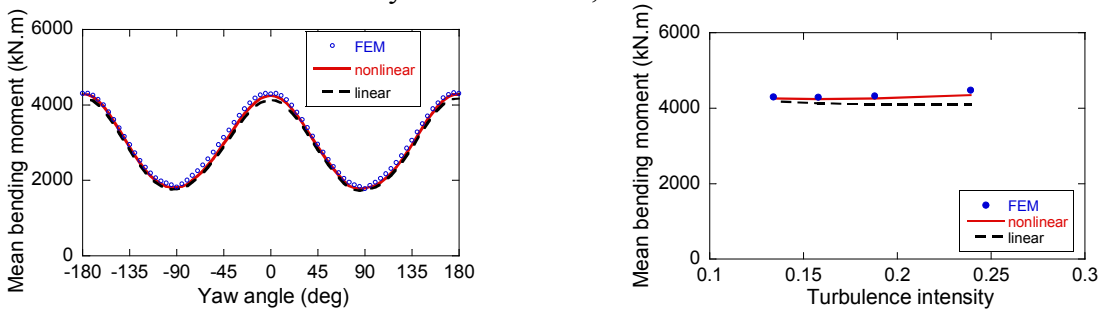

(a) For different yaw angles ($I_u = 0.158$ at hub height) (b) For different terrain categories ($\theta = 0^\circ$)

Figure 1. Comparison of mean bending moment (400kW).

2.2 *Standard deviation*

Both resonant and background standard deviation should include two components, which depend on the longitudinal and lateral wind fluctuation, respectively. By numerical simulation, it is found that σ_{MRDv} and σ_{MBDv} due to lateral wind fluctuation v can be neglected compared to σ_{MRDu} and σ_{MRDu} due to longitudinal wind fluctuation u. Hence, the resonant and background standard deviation can be expressed as

$$\sigma^2_{MRD} = \sigma^2_{MRDu} + \sigma^2_{MRDv} \doteq \sigma^2_{MRDu} = \left[2\frac{\overline{M}_D}{1+I_u^2} I_u \frac{\pi\phi_D}{\sqrt{4\pi\xi_D}}\sqrt{R_u(f)}\sqrt{K_{MRDu}(f)}\right]^2 \tag{3}$$

$$\sigma^2_{MBD} = \sigma^2_{MBDu} + \sigma^2_{MBDv} \doteq \sigma^2_{MBDu} = \left[2\frac{\overline{M}_D}{1+I_u^2} I_u \sqrt{K_{MBDu}}\right]^2 \tag{4}$$

where $R_u(f)$ is the power spectral density of longitudinal wind fluctuation u.

(a) Mode correction factor

Assuming that the tower has uniform mass distribution and diameter along its height, the integral calculation of mode correction factor ϕ_D can be simplified as Equation 5. A unified mode correction factor is obtained for different wind turbines and different terrain categories. The parameters γ_M, λ_a and λ_b are determined as the average of the results of different wind turbines of 100kW-2000kW, respectively. $c = 0.9$ is a correction factor due to the approximation during the simplification. Figure 2a shows a good agreement between the simplified formula and the integral calculation. ϕ_D varies with yaw angle in a range of 0.85-1.0, larger than 0.81 of tower, which means that the existence of rotor increases the mode correction factor.

$$\phi_D = \frac{\int U^2(r) C_D(r,\theta)\mu(r)c(r)dr}{\int U^2(r) C_D(r,\theta)c(r)rdr} \frac{\int m(r)\mu(r)rdr}{m_T} = c\cdot\gamma_M\cdot a\cdot b = 0.9\gamma_M\cdot a\cdot b \tag{5}$$

where

$$\gamma_M = \frac{m_s}{m_T} = 1.96, \qquad a = \frac{\int m(r)\mu(r)rdr}{m_s H} = \lambda_a a', \qquad b = \frac{C_D^r(\theta)A_r + \int_0^H C_D^t\left[\frac{U(z)}{U_H}\right]^2 d(z)\mu(z)dz}{C_D^r(\theta)A_r + \int_0^H C_D^t\left[\frac{U(z)}{U_H}\right]^2 d(z)\frac{z}{H}dz} = \lambda_b b'$$

$$\lambda_a = 2.32, \qquad \lambda_b = 1.25 + 0.07\cos 2\theta$$

$$a' = \frac{\int_0^H m(z)\mu(z)zdz}{m_t H} = \frac{1}{2+\beta_s} = 0.25 \quad (\beta_s = 2.0), \qquad b' = \frac{\int_0^H C_D^t\left[\frac{U(z)}{U_H}\right]^2 d(z)\mu(z)dz}{\int_0^H C_D^t\left[\frac{U(z)}{U_H}\right]^2 d(z)\frac{z}{H}dz} = 1 - 0.4\ln\beta_s = 0.72$$

where $m(r)$ is the mass per length of the element at position r, m_r and m_t are the mass of rotor and tower, respectively, m_s is the total mass of wind turbine, m_T is the generalized mass of the whole wind turbine, H is the hub height, U_H is the mean wind velocity at hub height, A_r is the rotor area, $C_D^r(\theta)$ is the equivalent aerodynamic coefficient for rotor, and C_D^t is the aerodynamic coefficient for tower.

(b) Size reduction factor

Referring to the resonant and background size reduction factors in AIJ (2004), the formula formats for lattice structures are adopted in this study for simplification, as shown in Equations 6 and 7, taking the rotor radius R as the characteristic size of the whole wind turbine. The non-dimensional decay factor $C = 8.0$ is used here. Figures 2b, c show a good agreement between the simplified formula and the integral calculation for each size reduction factor. Both resonant and background size reduction factors vary in the range of 0-1.0, and the background one decreases when the wind turbine size increases. However, the resonant one doesn't have this feature, since it is also related to the natural frequency of wind turbine.

$$K_{MRDu}(f) = \frac{\int\int \exp\left[-C|r-r'|f/U_H\right] C_D(r,\theta)C_D(r',\theta)c(r)c(r')\mu(r)\mu(r')drdr'}{\left(\int C_D(r,\theta)c(r)\mu(r)dr\right)^2} = \frac{1}{\left(1+0.26\frac{CfR}{U_H}\right)^2} \tag{6}$$

$$K_{MBDu} = \frac{\int\int \exp\left[-|r-r'|/0.3L_u\right] C_D(r,\theta)C_D(r',\theta)c(r)c(r')rr'drdr'}{\left(\int C_D(r,\theta)c(r)rdr\right)^2} = \frac{1}{1+0.69\frac{R}{0.3L_u}} \tag{7}$$

where L_u is the along-wind turbulence integral length scale.

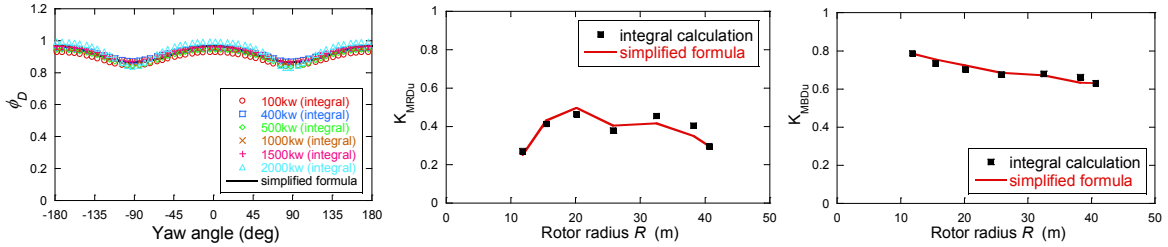

(a) Mode correction factor (b) Resonant one $K_{MRDu}(f)$ (c) Background one K_{MBDu}

Figure 2. Comparison of mode correction factor and size reduction factors.

(c) Damping ratio

The aerodynamic damping ratio ξ_{aD} can be simplified as Equation 8. The total damping ratio ξ_D is the summation of structural damping ratio ξ_s and aerodynamic damping ratio.

$$\xi_{aD}=\frac{\int \rho C_D(r,\theta)U(r)c(r)\mu^2(r)dr}{4\pi m_T f}=\frac{\rho U_H}{4\pi m_T f}\left(C_D^r(\theta)\cdot A_r+C_D^t\cdot H\cdot 0.16D_a\right) \tag{8}$$

$$\xi_D=\xi_s+\xi_{aD} \tag{9}$$

where $D_a=\left(D_{top}+D_{bottom}\right)/2$, D_{top} and D_{bottom} are the diameter of the top and bottom of tower, respectively. Figure 3a shows a good agreement with the integral calculation for aerodynamic damping ratio.

Using the equivalent aerodynamic coefficient instead of the actual one on rotor can generate some error, especially for resonant standard deviation. Therefore, a correction factor $f(\theta)=1/\sqrt{1.0+0.3\cos 2\theta}$ should be multiplied in the final simplified resonant standard deviation. Figure 3b shows a good agreement between the simplified formula, the integral calculation and FEM simulation for standard deviation.

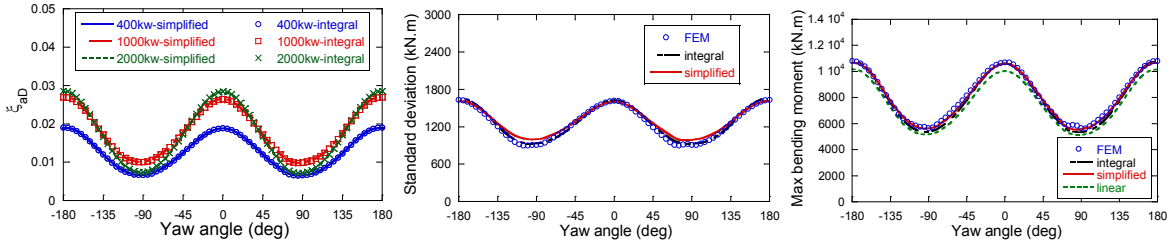

(a) Aerodynamic damping ratio (b) Standard deviation (400kW) (c) Maximum (400kW)

Figure 3. Comparison of aerodynamic damping ratio, standard deviation and maximum bending moment.

2.3 *Peak factor*

In order to take the non-linear component of wind load into account, Kareem et al. (1998) evaluated the peak factor for the non-Gaussian case by employing the moment-based Hermite transformation which has been shown to be accurate and robust. Binh et al. (2008) proved that the effect of kurtosis α_4 can be neglected since it is negligibly small compared to that of the second and third order from the order analysis of turbulence intensity I_u. α_4 is then assumed to be equal to the value of a Gaussian process (i.e., 0). Binh et al. (2008) proposed a formula of skewness α_3 for wind turbines as well, considering both significant resonant response and spatial correlation of wind load using a correlation coefficient $\rho(r,r')=\exp\left[-|r-r'|/0.3L_u\right]$. Finally, the non-Gaussian peak factor becomes Equation 10. For a Gaussian case, $\alpha_3=0$ which reduces this peak factor to the standard Gaussian form.

$$\begin{aligned} g_D&=\kappa\left\{\left(\beta+\frac{\gamma}{\beta}\right)+h_3\left(\beta^2+2\gamma-1\right)+h_4\left[\beta^3+3\beta(\gamma-1)+\frac{3}{\beta}\left(\frac{\pi^2}{12}-\gamma+\frac{\gamma^2}{2}\right)\right]\right\} \\ &=\kappa\left\{\left(\beta+\frac{\gamma}{\beta}\right)+h_3\left(\beta^2+2\gamma-1\right)\right\} \end{aligned} \tag{10}$$

where $\gamma=0.5772$, $\beta=\sqrt{2\ln\left(\nu_D' T\right)}$, $\kappa=\frac{1}{\sqrt{1+2h_3^2+6h_4^2}}=\frac{1}{\sqrt{1+2h_3^2}}$, $h_3=\frac{\alpha_3}{4+2\sqrt{1+1.5\alpha_4}}=\frac{\alpha_3}{6}$,

$h_4=\frac{\sqrt{1+1.5\alpha_4}-1}{18}=0$, $\nu_D'=\frac{1}{\kappa\sqrt{1+4h_3^2+18h_4^2}}\nu_D=\frac{1}{\kappa\sqrt{1+4h_3^2}}\nu_D$, $\alpha_3=\frac{1}{1.3R_D+1}\times\frac{3I_u a_{r1D}}{(K_{MBDu})^{3/2}}$,

$\nu_D=f\sqrt{\frac{(f_{0D}/f)^2+R_D}{1+R_D}}$, $f_{0D}=0.3\frac{U_H}{\sqrt{L_u\sqrt{A_{wt}}}}$, $R_D=\left(\frac{\sigma_{MRD}}{\sigma_{MBD}}\right)^2$,

$$a_{r1D}=\frac{\iiint \rho(r,r')\rho(r',r'')C_D(r,\theta)C_D(r',\theta)C_D(r'',\theta)c(r)c(r')c(r'')rr'r''drdr'dr''}{\left(\int C_D(r,\theta)c(r)rdr\right)^3}=\frac{1}{1+1.67\frac{R}{0.3L_u}},$$

ν'_D and ν_D are the zero up-crossing number in the estimated time interval T (normally 600s) of non-Gaussian process and Gaussian process, respectively, and A_{wt} is the wind acting area of the whole wind turbine.

Figure 3c shows how the maximum bending moment on the tower base of this study strongly correlates with the FEM simulation in arbitrary yaw angle. It is also noticed that the linear model underestimates the along-wind maximum bending moment obviously.

3 WIND LOAD FOR ACROSS-WIND DIRECTION

Equivalent static method is also applicable to across-wind direction.

$$M_L = \overline{M_L} + g_L \cdot \sigma_{ML} = \overline{M_L} + g_L \sqrt{\sigma_{MRL}^2 + \sigma_{MBL}^2} \tag{11}$$

3.1 *Mean bending moment*

The mean bending moment at the tower base can be calculated as:

$$\overline{M_L} = \int_{wt} \frac{1}{2} \rho C_L(r,\theta) c(r) U^2(r) \left[1 + I_u{}^2(r)\right] r dr \tag{12}$$

where $C_L(r,\theta)$ is the lift aerodynamic coefficient. Figure 4 shows a good agreement with FEM simulation and the effect of nonlinear wind pressure on the mean bending moment is not so significant as that of along-wind direction.

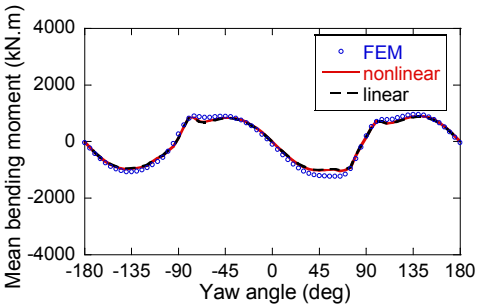

(a) For different yaw angles ($I_u = 0.158$ at hub height)

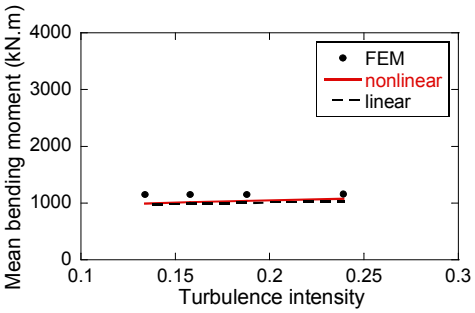

(b) For different terrain categories ($\theta = 70^\circ$)

Figure 4. Comparison of mean bending moment (400kW).

3.2 *Standard deviation*

For wind turbine, the across-wind mean bending moment $\bar{M}_L$ becomes close to zero at some yaw angles. In this study, the along-wind mean bending moment $\bar{M}_D$ is employed to calculate the across-wind standard deviation of bending moment. Unlike the along-wind direction, in both resonant and background standard deviation σ_{MRL} and σ_{MBL}, neither part caused by the two wind fluctuation components u and v can be neglected.

$$\sigma_{MRL}^2 = \sigma_{MRLu}^2 + \sigma_{MRLv}^2 = \left[\frac{2\overline{M}_D}{1+I_u^2}\frac{I_u \pi \phi_L}{\sqrt{4\pi\xi_L}}\sqrt{R_u(f)}\sqrt{K'_{MRLu}(f)}\right]^2 + \left[\frac{2\overline{M}_D}{1+I_u^2}\frac{I_v \pi \phi_L}{\sqrt{4\pi\xi_L}}\sqrt{R_v(f)}\sqrt{K'_{MRLv}(f)}\right]^2 \tag{13}$$

$$\sigma_{MBL}^2 = \sigma_{MBLu}^2 + \sigma_{MBLv}^2 = \left[2\frac{\overline{M}_D}{1+I_u^2} I_u \sqrt{K'_{MBLu}}\right]^2 + \left[2\frac{\overline{M}_D}{1+I_u^2} I_v \sqrt{K'_{MBLv}}\right]^2 \tag{14}$$

where $R_v(f)$ is the power spectral density of lateral wind fluctuation v.

(a) Mode correction factor

The mode correction factor ϕ_L is the same as that of along-wind direction

$$\phi_L = \phi_D \tag{15}$$

(b) Size reduction factor

The correlation factors $K'_{MRLu}(f), K'_{MRLv}(f), K'_{MBLu}, K'_{MBLv}$ in across-wind direction can be written as the product of conventional size reduction factor and wind force ratio, as shown in Equations 16-19. The conventional size reduction factors can be simplified by the same approach as that for along-wind direction.

$$K'_{MRLu}(f) = K_{MRLu}(f)\cdot\beta_{Ru}$$

$$= \frac{\int\int \exp\left[-C|r-r'|f/U_H\right] C_L(r,\theta)C_L(r',\theta)c(r)c(r')\mu(r)\mu(r')drdr'}{\left(\int C_L(r,\theta)c(r)\mu(r)dr\right)^2} \cdot \frac{\left(\int C_L(r,\theta)c(r)\mu(r)dr\right)^2}{\left(\int C_D(r,\theta)c(r)\mu(r)dr\right)^2} \tag{16}$$

$$= \frac{1}{\left(1+0.21\dfrac{CfR}{U_H}\right)^2}\cdot\left(\frac{C_L^r(\theta)\cdot a_R}{1+C_D^r(\theta)\cdot a_R}\right)^2, \qquad a_R = \frac{A_r}{0.18D_aH}$$

$$K'_{MRLv}(f) = K_{MRLv}(f)\cdot\beta_{Rv}$$

$$= \frac{\int\int \exp\left[-C|r-r'|f/U_H\right] A_L(r,\theta)A_L(r',\theta)c(r)c(r')\mu(r)\mu(r')drdr'}{\left(\int A_L(r,\theta)c(r)\mu(r)dr\right)^2} \cdot \frac{\left(\int A_L(r,\theta)c(r)\mu(r)dr\right)^2}{\left(\int C_D(r,\theta)c(r)\mu(r)dr\right)^2} \tag{17}$$

$$= \frac{1}{\left(1+0.21\dfrac{CfR}{U_H}\right)^2}\cdot\left(\frac{A_L^r(\theta)\cdot a_R}{1+C_D^r(\theta)\cdot a_R}\right)^2$$

$$K'_{MBLu} = K_{MBLu}\cdot\beta_{Bu}$$

$$= \frac{\int\int \exp\left[-|r-r'|/0.3L_u\right] C_L(r,\theta)C_L(r',\theta)c(r)c(r')rr'drdr'}{\left(\int C_L(r,\theta)c(r)rdr\right)^2} \cdot \frac{\left(\int C_L(r,\theta)c(r)rdr\right)^2}{\left(\int C_D(r,\theta)c(r)rdr\right)^2} \tag{18}$$

$$= \frac{1}{1+0.5\dfrac{R}{0.3L_u}}\cdot\left(\frac{C_L^r(\theta)\cdot a_B}{1+C_D^r(\theta)\cdot a_B}\right)^2, \qquad a_B = \frac{A_r}{0.28D_aH}$$

$$K'_{MBLv} = K_{MBLv}\cdot\beta_{Bv}$$

$$= \frac{\int\int \exp\left[-|r-r'|/0.3L_v\right] A_L(r,\theta)A_L(r',\theta)c(r)c(r')rr'drdr'}{\left(\int A_L(r,\theta)c(r)rdr\right)^2} \cdot \frac{\left(\int A_L(r,\theta)c(r)rdr\right)^2}{\left(\int C_D(r,\theta)c(r)rdr\right)^2} \tag{19}$$

$$= \frac{1}{1+0.5\dfrac{R}{0.3L_v}}\cdot\left(\frac{A_L^r(\theta)\cdot a_B}{1+C_D^r(\theta)\cdot a_B}\right)^2$$

where $A_L(r,\theta) = 0.5\left[C_D(r,\theta) + \partial C_L(r,\theta)/\partial\theta\right]$, $C_L^r(\theta)$ and $A_L^r(\theta)$ are the equivalent aerodynamic coefficients for rotor in the across-wind direction and L_v is the across-wind turbulence integral length scale. Figure 5 shows a good agreement between the simplified formula and the integral calculation for each size reduction factor.

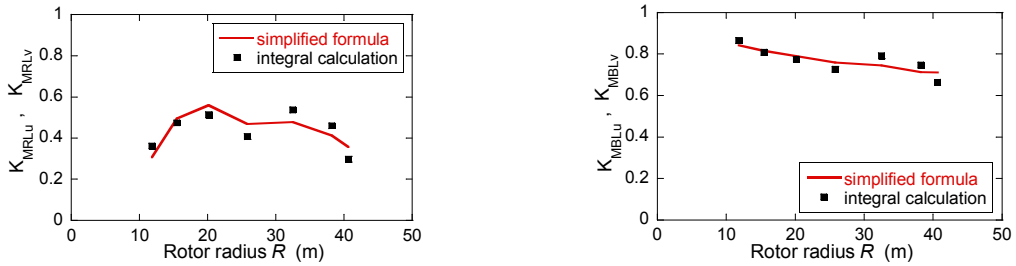

(a) Resonant size reduction factor $K_{MRLu}(f), K_{MRLv}(f)$ (b) Background size reduction factor K_{MBLu}, K_{MBLv}

Figure 5. Comparison of size reduction factors.

(c) Damping ratio

It should be noted that for across-wind direction, since the aerodynamic damping ratio ξ_{aL} may become negative at some yaw angle, Equation 21 is used to limit the total damping ratio ξ_L not less than the structural damping ratio in order to avert an unstable response.

$$\xi_{aL} = \frac{\int \rho A_L(r,\theta) U(r) c(r) \mu^2(r) dr}{4\pi m_T f} = \frac{\rho A_L^r(\theta) U_H A_r}{4\pi m_T f} \tag{20}$$

$$\xi_L = \max\left(\xi_s + \xi_{aL}, \xi_s\right) \tag{21}$$

Figure 6a shows a good agreement between the simplified formula and the integral calculation for aerodynamic damping ratio. Figure 6b shows a good agreement between the simplified formula, the integral calculation and FEM simulation for standard deviation.

3.3 *Peak factor*

For the across wind response, the Gaussian peak factor is used in this study and is expressed as

$$g_L = \sqrt{2\ln(600\nu_L)} + \frac{0.5772}{\sqrt{2\ln(600\nu_L)}} \tag{22}$$

where $\nu_L = f\sqrt{\frac{(f_{0L}/f)^2 + R_L}{1+R_L}}$, $f_{0L} = 0.3\frac{U_H}{\sqrt{L_v\sqrt{A_{wt}}}}$, $R_L = \left(\frac{\sigma_{MRL}}{\sigma_{MBL}}\right)^2$.

Figure 6c shows how the maximum bending moment on the tower base of this study strongly correlates with the FEM simulation in arbitrary yaw angle.

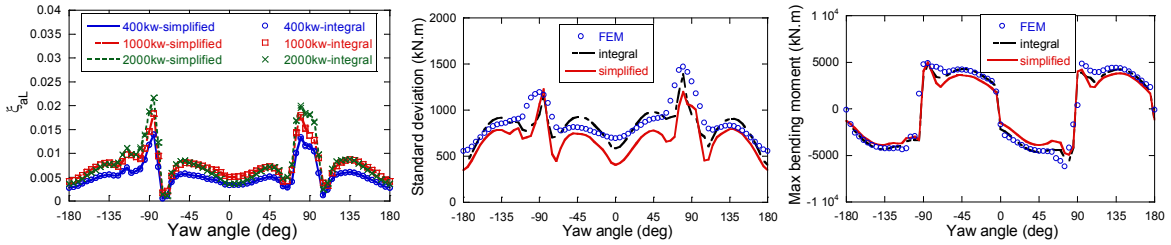

(a) Aerodynamic damping ratio b) Standard deviation (400kW) (c) Maximum (400kW)

Figure 6. Comparison of aerodynamic damping ratio, standard deviation and maximum bending moment.

4 COMBINATION OF WIND LOADS

It has been noticed that the maximum values of along wind and across wind loads can't occur simultaneously. Hence, the correlation coefficient of wind responses in the two directions should be considered. Referring to Asami (2000), the maximum wind load acting on the tower for any yaw angle can be estimated as

$$M_{DL} = \max\left(\sqrt{M_L^2 + \left(\bar{M}_D + \gamma_{DL}(M_D - \bar{M}_D)\right)^2}, \sqrt{M_D^2 + \left(\bar{M}_L + \gamma_{DL}(M_L - \bar{M}_L)\right)^2}\right) \tag{23}$$

where $\gamma_{DL} = \sqrt{2+2\rho_{DL}} - 1$, ρ_{DL} is the correlation coefficient between along wind and across wind responses, which can be determined by Table 1 for stall-regulated wind turbines. Figure 7 shows the comparison of the simplified formula, and FEM simulation. It is obvious that for any yaw angle, the correlation coefficients shown in Table 1 give a good agreement with FEM simulation. It is also noticed that the uncorrelated approximation (ρ_{DL} = 0) underestimates the maximum bending moment, while for the yaw angle range of ±90°±15°, completely correlated approximation(ρ_{DL} = 1) gives a significantly conservative result, with the error of nearly 20% at maximum.

Table 1. Correlation coefficients between along wind and across wind responses

	θ (deg)	ρ_{DL}
(1)	-180 ~ -110 -80 ~ 70 100 ~ 180	1.0
(2)	-90, 80	0.0
(3)	-110 ~ -90 -90 ~ -80 70 ~ 80 80 ~ 100	linear interpolation between (1) and (2)

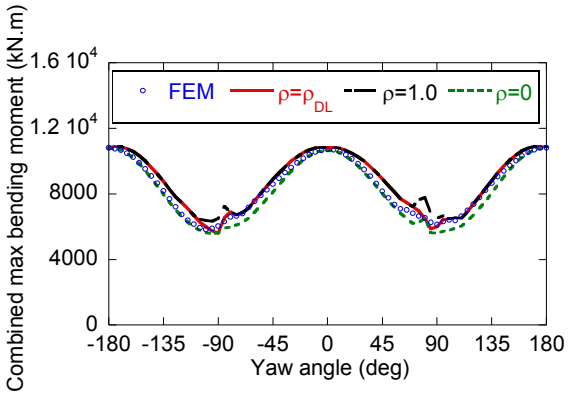

Figure 7. Comparison of combined maximum bending moment (400kW).

5 CONCLUSIONS

In this study, the wind load evaluation formulas of both along-wind direction and across-wind direction are proposed for arbitrary yaw angle. The complex integrals of some critical parameters are simplified. Though the simplification, a unified mode correction factor is proposed. It varies with yaw angle in a range of 0.85-1.0, larger than that of tower due to the existence of rotor. Both resonant and background size reduction factors vary in the range of 0-1.0, and the background one decreases when the wind turbine size increases. However, the resonant one doesn't have this feature, since it is also related to the natural frequency of wind turbine. A new non-Gaussian peak factor model is proposed for along-wind direction, which can be reduced to the conventional Gaussian form for a Gaussian case. A formula for the combination of along wind and across wind loads is proposed to calculate the final design wind load considering the correlation coefficient in the two directions. It is also noticed that the uncorrelated approximation underestimates the maximum bending moment, while for the yaw angle range of ±90°±15°, completely correlated approximation gives a significantly conservative result. All the proposed formulas have been verified using FEM simulation.

REFERENCES

Architectural Institute of Japan (AIJ), 2004. Recommendations for loads on buildings.

Asami, Y., 2000. Wind loads combination for high-rise building. 16th Symposium on Wind Engineering, 531-534. (in Japanese)

Burton, T., Sharpe, D., Jenkins, N., Bossanyi, E., 2001. Wind energy handbook. WILEY, England.

Binh, L.V., Ishihara, T., Phuc, P.V., Fujino, Y., 2008. A peak factor for non-Gaussian response analysis of wind turbine tower. Journal of Wind Engineering and Industrial Aerodynamics 96, 2217-2227.

International Electrotechnical Commission, 2005. International Standard: Wind turbines – Part 1: Design requirements, IEC 61400-1, Edition 3.0, Geneva.

Ishihara, T., Yamaguchi, A., Takahara, K., Mekaru, T., Matsuura, S., 2005a. An analysis of damaged wind turbines by Typhoon Maemi in 2003. Proceedings of 6th Asia-Pacific Conference on Wind Engineering, 1413-1428.

Ishihara, T., Phuc, P.V., Fujino, Y., Takahara, K., Mekaru, T., 2005b. A field test and full dynamic simulation on a stall regulated wind turbine. Proceedings of 6th Asia-Pacific Conference on Wind Engineering, 599-612.

Ishihara, T., 2007. Guidelines for design of wind turbine support structures and foundations. Japan Society of Civil Engineers, Tokyo. (in Japanese)

Kareem, A., Tognarelli, M.A., Gurley, K.R., 1998. Modeling and analysis of quadratic term in the wind effects on structures. Journal of Wind Engineering and Industrial Aerodynamics 74-76, 1101-1110.